Homoleptic $[ONO]_2Ti(IV)$ Type Complexes of Amino-Acid-Tethered Phenolato, Schiff-Base Ligands: Synthesis, Characterization, Time-Resolved Fluorescence Spectroscopy, and Cytotoxicity against Ovarian and Colon Cancer Cells

Zohar Shpilt,[a†] Rajesh Manne,[b†] Mostofa Ataur Rohman,[b] Sivaprasad Mitra,[b] Edward R. T. Tiekink,*[c] Tushar S. Basu Baul,*[b] Edit Y. Tshuva.*[a]

[†] *These individuals contributed equally to this manuscript.*

[a] *Institute of Chemistry, The Hebrew University of Jerusalem, Jerusalem 9190401, Israel. Email: edit.tshuva@mail.huji.ac.il*

[b] *Centre of Advanced Studies in Chemistry, North-Eastern Hill University, NEHU Permanent Campus, Umshing, Shillong 793 022, India. Email: basubaul@nehu.ac.in, basubaulchem@gmail.com*

[c] *Research Centre for Crystalline Materials, School of Science and Technology, Sunway University, 47500 Bandar Sunway, Selangor Darul Ehsan, Malaysia. Email: edwardt@sunway.edu.my, edward.tiekink@gmail.com*

*†CCDC-1869232-1869235 contain the supplementary crystallographic data for compounds **1**, **2**, **5**, and **6**, respectively, and CCDC-1891900 contains the supplementary crystallographic data for compound **3**. These data can be obtained free of charge from The Cambridge Crystallographic Data Centre via www.ccdc.cam.ac.uk/data_request/cif.*

Electronic supplementary information (ESI) available.

Abstract

Six homoleptic Ti(IV) compounds of dianionic tridentate Schiff base ligands were synthesized from chiral amino acids, 2-hydroxybenzaldehyde and $Ti(OiPr)_4$. The compounds were spectroscopically characterized and the molecular geometries were established by X-ray crystallography. The ligands coordinated ~~the~~ titanium via carboxylate-O-, imine-N-, and phenoxide-O atoms. Two isomers were identified; each based on a *trans*-N_2O_4 donor set, but one with *trans* carboxylate-O atoms and another with each carboxylate-O atom *trans* to a phenoxide-O atom. Photophysical profiles exhibited faster excited-state relaxation in the solid phase than in solution. Marked cytotoxicities were recorded toward human ovarian A2780 and colon HT-29 cancer cells with IC_{50} values ranging between 23±2 and 103±3 μM. Comparative hydrolytic stability studies by NMR in 10% D_2O solutions provided $t_{1/2}$ values of up to 15±2 h, with little correlation to cytotoxicity implying a role of hydrolysis products in the reactivity and identifying steric bulk as a contributor to stability and solubility.

Keywords

cytotoxicity, metallodrugs, O-ligands, Ti(IV), Schiff-base ligands

Introduction

The licensing of cisplatin in the 1970s ~~has~~ initiated a widespread search for other anticancer metallodrugs that could overcome its toxicity and acquired-resistance properties.[1–3] Other metals were proposed, among which titanium is a promising candidate due to its biocompatibility.[4-25] Two titanium(IV)-based complexes, budotitane and titanocene dichloride, were the first non-platinum metallodrugs to enter clinical trials. They failed due to low water solubility and rapid hydrolysis, which required high doses of administration ultimately leading to insufficient efficiency.[26,27]

Our group has introduced a new class of Ti(IV) complexes, based on phenolato ligands. The first generation comprised diaminobis(phenolato) tetradentate ligands, with two labile alkoxo ligands per metal center.[28] The complexes of this class exhibited *in vitro* and *in vivo* cytotoxicity toward cancer cells and relatively high hydrolytic stability, and were therefore widely explored.[29-47] Further stabilization was achieved upon the employment of hexadentate derivatives of the phenolato ligands, leading to highly cytotoxic complexes that were stable for weeks in water.[34,48–52] These observations, along with other reports of inert Ti(IV) complexes with anticancer properties,[53–55] indicate that the labile ligands are not required for antiproliferative effects. Consequently, we have recently reported the synthesis of eight Ti(IV) complexes with two dianionic tridentate acylhydrazone ligands, which showed high hydrolytic stability and cytotoxicity comparable to that of cisplatin.[56]

Amino acids and their derivatives have been extensively used as ligands in metal complexes for various purposes, such as catalysis, labeling, amino acid and peptide synthesis, and pharmaceutical applications.[57] Specifically, the use of amino acids in ligands for anticancer metal complexes has been established since the clinical development of cisplatin, for two main reasons.[58] First, amino acids are biological materials that enter cells through active-transport mechanisms,[59,60] making the complexes biocompatible and reducing the chances for developing resistance. Second, given the extensive proliferative rates of cancer cells, their requirements for

metabolites such as amino acids are greater than the needs of normal cells, which may cause cancer cells to mistake the ligands for natural amino acids, hindering further proliferation.[61–63] Numerous examples of amino acid-based anticancer metal complexes exist in the literature, including titanium,[64] zirconium,[65] palladium,[66] ruthenium,[67] and tin complexes.[68–71]

Herein, we present six novel Ti(IV) complexes, all composed of tridentate amino acid-tethered phenolato ligands. The amino acids applied in this study were of a hydrophobic nature, in the hope of accelerating the penetration of cellular membranes by the complexes. We describe the synthesis and characterization of the complexes and analyze their hydrolytic stability and cytotoxicity toward two cancer cell lines.

Experimental section

Materials and physical measurements

Titanium(IV) tetra(isopropoxide), L-alanine, L-valine, L-isoleucine, L-leucine, D,L-phenylalanine, L-tryptophan, salicylaldehyde were purchased from SRL and used without further purification. Solvents used were of A. R. grade and dried using standard procedures. Benzene, toluene and hexane were distilled from benzophenone/sodium, whereas methanol and dichloromethane were distilled over activated magnesium and calcium hydride, respectively. All manipulations were performed using standard Schlenk lines in an atmosphere of dry dinitrogen or argon, unless otherwise stated. Note: Reactions can be conducted in toluene, however, synthetic conveniences, particularly the higher boiling point of toluene, led to the choice of benzene. Care in handling benzene should be exercised.

Melting points were measured using a Büchi M-560 instrumentation. Elemental analyses were performed using a Perkin Elmer 2400 series II instrument. IR spectra in the range 4000-400 cm^{-1} were obtained as KBr discs on a Bruker ALPHA II FT-IR

spectrophotometer. Solution ^{1}H and $^{13}C\{^{1}H\}$ NMR spectra in $CDCl_3$, measured at 400.13 and 100.62 MHz respectively, were recorded on a Bruker AMX 400 spectrometer. The ^{1}H and ^{13}C chemical shifts were referenced to Me_4Si (δ 0.00 ppm) and $CDCl_3$ (δ 77.00 ppm), respectively. The UV-visible absorption and fluorescence measurements of the samples dissolved in spectroscopic grade DMSO and acetonitrile (concentration ca. 50 μM) were taken in PerkinElmer model Lambda25 and Quanta master (QM-40) steady-state fluorescence apparatus supplied by Photon Technology International (PTI), respectively. Spectra were calibrated by subtracting the solvent as blank control measured in the same condition. Photoluminescence spectra in the solid-state were measured by using a special solid-state sample holder (part no. 557820058) supplied by PTI in the same instrument. Fluorescence lifetime measurements of the samples were performed by exciting either at 295 nm or 365 nm in an LED-based time-correlated single photon counting (TCSPC) system (PM-3) supplied by PTI. The fluorescence decay spectra of the samples were collected at magic angles. Other details pertaining to fluorescence experiments and calculations are given in the supplementary materials (ESI Text S1).

Synthesis of titanium(IV) complexes 1-6

Titanium(IV) complexes **1**-**6** (Scheme 1) were prepared by separately reacting amino acids (L-alanine, L-valine, L-isoleucine, L-leucine, D,L-phenylalanine and L-tryptophan), 2-hydroxybenzaldehyde and titanium(IV) tetra(isopropoxide) in 2:2:1 molar ratio. Complexes **1**-**6** were prepared following a similar synthetic route and hence a detailed typical procedure for **1** is outlined below.

Synthesis of 1. Titanium(IV) tetra(isopropoxide) (0.25 g, 0.879 mmol) was added drop-wise to a stirred benzene suspension (30 ml) containing finally ground L-alanine (0.15 g, 1.759 mmol) and 2-hydroxybenzaldehyde (0.21 g, 1.758 mmol). The reaction

mixture slowly turned pale yellow, followed by heating to reflux for 45 minutes at 80 °C on an oil bath with continuous stirring. To this reaction mixture, 5 ml of methanol was added to aid the solubility and reflux was continued for an additional 8 h. A clear orange solution was filtered while hot and the filtrate was concentrated under reduced pressure. Pasty material was boiled with hexane, filtered, and the solid mass was dried *in vacuo*. The yellow powder was dissolved in 5 ml of hot chloroform, filtered, and the filtrate was concentrated up to 2 ml, which was precipitated with hexane. The precipitate was filtered, washed several times with hot hexane, and dried *in vacuo*. Recrystallization from a benzene/ methanol mixture (3:1 ratio) afforded orange crystals suitable for single crystal XRD. Yield: 0.28 g, 74%. m.p. 303-306 °C; ^{1}H NMR (400 MHz, $CDCl_3$): δ=8.51 (s, 2H; H-7), 7.52-7.44 (m, 4H; H-3 and H-5), 7.00 (t, 2H; H-4), 6.65 (d, 2H; H-2), 4.68 (q, 2H; H-9), 1.69 ppm (d, $^{3}J_{H,H}$=8 Hz, 6H; H-11); ^{13}C NMR (100 MHz, $CDCl_3$): δ=176.4 (C-10), 165.1 (C-7), 162.3 (C-1), 137.3 (C-3), 134.4 (C-5), 122.2 (C-6), 121.8 (C-2), 115.8 (C-4), 71.0 (C-9), 21.6 ppm (C-11); IR (KBr): $\tilde{\nu}$=1696 $(OCO)_{asym}$, 1608 (C=N), 1551, 1474, 1448, 1396 $(OCO)_{sym}$, 1370, 1290, 1246, 1156, 1130, 1051, 912, 822, 759, 645, 566 cm^{-1}; elemental analysis calcd (%) for $C_{20}H_{18}N_2O_6Ti$: C 55.83, H 4.22, N 6.51; found: C 56.13, H 4.44, N 6.14.

Synthesis of 2. An analogous method to that used for the preparation of **1** was followed using titanium(IV) tetra(isopropoxide) (0.25 g, 0.879 mmol), L-valine (0.20 g, 1.759 mmol) and 2-hydroxybenzaldehyde (0.21 g, 1.758 mmol), giving orange crystals of **2** from a toluene/ dichloromethane/ methanol (v/v, 2:1:1) mixture in a yield of 0.31g, 72%. The crystals turned into powder with time. For diffraction studies, crystals of **2** were recrystallized from ethanol and stored in silicon oil. m.p. 309-312 °C; ^{1}H NMR (400 MHz, $CDCl_3$): δ=8.43 (s, 2H; H-7), 7.54-7.49 (m, 4H; H-3 and H-5), 7.02 (t, 2H; H-4), 6.60 (d, 2H; H-2), 4.39 (d, 2H; H-9), 2.33 (m, 2H; H-11), 1.11 (d, $^{3}J_{H,H}$=6.8 Hz, 6H; H-12a), 1.06 ppm (d, $^{3}J_{H,H}$=6.8 Hz, 6H; H-12b); ^{13}C NMR (100 MHz,

$CDCl_3$): δ=174.8 (C-10), 165.6 (C-7), 162.4 (C-1), 137.3 (C-3), 134.6 (C-5), 122.4 (C-2), 121.8 (C-4), 115.7 (C-6), 80.9 (C-9), 36.0 (C-11), 18.7 (C-12a), 18.3 ppm (C-12b) ppm; IR (KBr): $\tilde{\nu}$=1701 $(OCO)_{asym}$, 1605 (C=N), 1551, 1470, 1446, 1399 $(OCO)_{sym}$, 1284, 1152, 1126, 1031, 906, 820, 762, 643, 594, 567 cm^{-1}; elemental analysis calcd (%) for $C_{24}H_{26}N_2O_6Ti$: C 59.27, H 5.39, N 5.76; found: C 59.55, H 5.98, N 5.30.

Synthesis of 3. An analogous method to that used for the preparation of **1** was followed using titanium(IV) tetra(isopropoxide) (0.25 g, 0.879 mmol), L-isoleucine (0.23 g, 1.759 mmol) and 2-hydroxybenzaldehyde (0.21 g, 1.758 mmol), giving orange crystals of **3** from a chloroform/ethanol (v/v, 3:1) mixture in a yield of 0.32 g, 70%. The crystals turned into powder with time. For diffraction studies, crystals of **3** were recrystallized from ethanol and stored in silicon oil. m.p. 292-295 °C; ^{1}H NMR (400 MHz, $CDCl_3$): δ=8.43 (s, 2H; H-7), 7.54-7.48 (m, 4H; H-3 and H-5), 7.02 (t, 2H; H-4), 6.60 (d, 2H; H-2), 4.49 (d, 2H; H-9), 1.96 (m, 2H; H-11), 1.73-1.68 (m, 2H; H-12a), 1.47-1.41 (m, 2H; H-12b), 1.05 (d, $^3J_{H,H}$= 6.5 Hz, 6H; H-14), 0.94 ppm (t, $^3J_{H,H}$= 7 Hz, 6H; H-13). ^{13}C NMR (100 MHz, $CDCl_3$): δ=174.5 (C-10), 165.3 (C-7), 162.4 (C-1), 137.1 (C-3), 134.5 (C-5), 122.4 (C-2), 121.7 (C-4), 115.6 (C-6), 79.6 (C-9), 43.7 (C-11), 25.8 (C-12), 14.7 (C-14), 12.1 ppm (C-13); IR (KBr): $\tilde{\nu}$=1699 $(OCO)_{asym}$, 1604 (C=N), 1550, 1445, 1402 $(OCO)_{sym}$, 1285, 1231, 1152, 1127, 969, 943, 828, 760, 641, 569 cm^{-1}; elemental analysis calcd (%) for $C_{26}H_{30}N_2O_6Ti$: C 60.71, H 5.88, N 5.45; found: C 61.22, H 5.80, N 5.55.

Synthesis of 4. An analogous method to that used for the preparation of **1** was followed using titanium(IV) tetra(isopropoxide) (0.25 g, 0.879 mmol), L-leucine (0.23 g, 1.759 mmol) and 2-hydroxybenzaldehyde (0.21 g, 1.758 mmol), giving orange crystals of **4** from ethanol in a yield of 0.29 g, 64%. The crystals turned into powder with time. For diffraction studies, crystals of **4** were stored in silicon oil. m.p. 202-204 °C; ^{1}H NMR (400 MHz, $CDCl_3$): δ=8.44 (s, 2H; H-7), 7.61-7.57 (m, 4H; H-3 and H-5), 7.12-7.08 (m, 2H; H-4), 6.71 (d, 2H; H-2), 4.64 (m, 2H; H-9), 2.07 (m, 2H; H-11), 1.87

(m, 4H; H-12), 1.03 ppm (brd, 12H; H-13a and 13b); ^{13}C NMR (100 MHz, $CDCl_3$): δ=175.1 (C-10), 164.0 (C-7), 161.8 (C-1), 136.8 (C-3), 133.9 (C-5), 121.7 (C-2), 121.4 (C-4), 115.3 (C-6), 73.9 (C-9), 44.1 (C-12), 23.4 (C-11), 22.3 (C-13b), 22.1 ppm (C-13a); IR (KBr): $\tilde{\nu}$=1699 $(OCO)_{asym}$, 1607 (C=N), 1551, 1470, 1446, 1399 $(OCO)_{sym}$, 1283, 1151, 1124, 913, 865, 820, 759, 641, 571 cm^{-1}; elemental analysis calcd (%) for $C_{26}H_{30}N_2O_6Ti$: C 60.71, H 5.88, N 5.45; found: C 61.10, H 6.02, N 5.44.

Synthesis of 5. An analogous method to that used for the preparation of **1** was followed using titanium(IV) tetra(isopropoxide) (0.25 g, 0.879 mmol), D,L-phenylalanine (0.29 g, 1.759 mmol) and 2-hydroxybenzaldehyde (0.21 g, 1.758 mmol), giving fine orange crystals of **5** (m.p. 268-270 °C) from a chloroform/hexane (v/v, 3:1) mixture. These crystalline materials were recrystallized from toluene, which provided diffraction quality crystals in a yield of 0.35 g, 68% . The crystals turned into powder with time. For diffraction studies, crystals of **5** were stored in silicon oil. m.p. 298-300 °C; ^{1}H NMR (400 MHz, $CDCl_3$): δ=8.27 (s, 2H; H-7), 7.62 (t, 2H; H-3), 7.48 (d, 2H; H-5), 7.25 (m, 6H; H-14, H-15 and H-16), 7.15 (m, 4H; H-13 and H-17), 7.08 (t, 2H; H-4), 6.65 (d, 2H; H-2), 4.97 (q, 2H; H-9), 3.48 (dd, 2H; H-11a), 3.14 ppm (dd, 2H, H-11b); ^{13}C NMR (100 MHz, $CDCl_3$): δ=175.0 (C-10), 164.8 (C-7), 162.1 (C-1), 137.1 (C-3), 135.7 (C-12), 134.2 (C-5), 130.3 (C-14 and C-16), 129.1 (C-13 and C-17), 127.6 (C-15), 121.9 (C-2), 121.6 (C-4), 115.7 (C-6), 78.1 (C-9), 40.9 ppm (C-11); IR (KBr): $\tilde{\nu}$=1695 $(OCO)_{asym}$, 1608 (C=N), 1551, 1473, 1445, 1400 $(OCO)_{sym}$, 1287, 1152, 1126, 1082, 914, 879, 840, 819, 758, 701, 639, 564 cm^{-1}; elemental analysis calcd (%) for $C_{32}H_{26}N_2O_6Ti$: C 65.99, H 4.50, N 4.81; found: C 65.78, H 4.80, N 4.80.

Synthesis of 6·C_6H_6. An analogous method to that used for the preparation of **1** was followed using titanium(IV) tetra(isopropoxide) (0.25 g, 0.879 mmol), L-tryptophan (0.36 g, 1.759 mmol) and 2-hydroxybenzaldehyde (0.21 g, 1.758 mmol), giving red crystals of **6** in a yield of 0.39 g, 67%. m.p. 283-286 °C; ^{1}H NMR (400 MHz, $CDCl_3$): δ=10.9 (s, 2H; H-14), 7.99 (s, 2H; H-7), 7.43 (t, 2H; H-3), 7.38 (d, 2H; H-5), 7.30-6.80

(m, 16H; H-13, H-17, H-18, H-19, H-20, and C_6H_6 solvate), 6.71 (t, 2H; H-4), 6.46 (d, 2H; H-2), 4.75 (q, 2H; H-9), 3.46 (dd, 2H; H-11a), 3.15 ppm (dd, 2H; H-11b); ^{13}C NMR (100 MHz, $CDCl_3$): δ=174.7 (C-10), 163.5 (C-1), 160.8 (C-7), 135.7, 133.2, 127.4 (C_6H_6 solvate), 125.9, 124.2, 120.9, 120.8, 120.6, 118.5, 117.4, 114.4, 110.9, 107.4 (ArC), 75.6 (C-9), 30.1 ppm (C-11); IR (KBr): $\tilde{\nu}$=3416 (N-H), 1688 $(OCO)_{asym}$, 1606 (C=N), 1549, 1442, 1426, 1393 $(OCO)_{sym}$, 1309, 1276, 1225, 1150, 1125, 1099, 898, 822, 770, 750, 682, 640, 568 cm^{-1}; elemental analysis calcd (%) for $C_{42}H_{34}N_4O_6Ti$: C 68.30, H 4.64, N 7.59; found: C 68.33, H 4.88, N 7.60.

Single crystal X-ray structure determination

For diffraction studies, crystals were stored in silicon oil to avoid crystal deterioration by efflorescent de-solvation. Crystal data and refinement details for **1**-**3**, **5**, and **6** are included in Table 1. Intensity data for the investigated complexes were measured at room temperature on an Agilent Xcalibur Eos Gemini diffractometer equipped with a CCD area detector and graphite-monochromated Mo Kα radiation (λ = 0.71073 Å). Data reduction and empirical absorption corrections, based on a multi-scan technique, were applied.[72] The structures were solved by direct methods,[73] and refined on F^2 with anisotropic displacement parameters and C-bound H atoms in the riding model approximation.[74] For **6**, the nitrogen-bound H atom was refined with a distance restraint N–H = 0.86 ± 0.01 Å. A weighting scheme of the form $w = 1/[\sigma^2(F_o^2) + (aP)^2 + bP]$ where $P = (F_o^2 + 2F_c^2)/3$) was introduced in each refinement. A consequence of the structures being determined at room temperature was the presence of large displacement parameters. Nevertheless, the structures were determined unambiguously and are in accord with the spectroscopic data. In the refinement of **1**, the methane-C2–C3(methyl) residue was statistically disordered and each component was refined anisotropically. For **2**, the C15-isopropyl group was statistically disordered. While each component was refined anisotropically, the

displacement ellipsoids were restrained to be nearly isotropic. The atoms of the C27-isopropyl group were also restrained to be nearly isotropic. Owing to poor agreement, one reflection, i.e. (3 0 3), was omitted from the final cycles of refinement. The absolute structures for **2** and **3** were determined based on differences in Friedel pairs included in the data set. At the conclusion of the refinement of **3**, evidence for disordered solvent was found, as was the presence of voids large enough to accommodate solvent. This electron density was modeled with the MASK routine of OLEX^2;[75] refer to the respective CIF for more details. For **6**, the absolute structure was determined as for **2** and **3**, and the N-bound H atom was refined with the distance restraint N–H = 0.86 ± 0.01 Å and with U_{iso} = 1.2 U_{eq}(N). The molecular structure diagrams were generated at the 25% probability level by ORTEP for Windows,[76] and the packing diagrams were generated with DIAMOND.[77] Additional data analysis was made with PLATON.[78]

Table 1. Crystal data and refinement details for **1**-**3**, **5**, and **6**.

	1	**2**	**3** [a]	**5**	**6**
Formula	$C_{20}H_{18}N_2O_6Ti$	$C_{24}H_{26}N_2O_6Ti$	$C_{26}H_{30}N_2O_6Ti$	$C_{32}H_{26}N_2O_6Ti$	$C_{36}H_{28}N_4O_6Ti.C_6H_6$
Formula weight	430.26	486.34	514.42	582.45	738.63
Crystal colour	orange	orange	orange	orange	red
Crystal size/mm^3	0.21 x 0.23 x 0.25	0.12 x 0.15 x 0.23	0.22 × 0.23 × 0.23	0.10 x 0.23 x 0.25	0.19 x 0.20 x 0.25
Crystal system	Monoclinic	Orthorhombic	Orthorhombic	Monoclinic	Tetragonal
Space group	*C*2/*c*	$P2_12_12_1$	$P2_12_12_1$	$P2_1/n$	$P4_32_12$
a/Å	18.0072(12)	11.5943(7)	11.5160(3)	11.8347(8)	10.8554(5)
b/Å	8.5565(6)	19.7512(16)	20.6532(5)	10.3845(8)	10.8554(5)
c/Å	12.9611(6)	21.7374(19)	23.1511(6)	22.7080(17)	30.210(2)
α/°	90	90	90	90	90
β/°	100.182(5)	90	90	98.975(7)	90
γ/°	90	90	90	90	90
V/Å^3	1965.6(2)	4977.9(7)	5506.3(3)	2756.6(4)	3559.9(4)
Z	4	8	8	4	4
D_c/g cm^{-3}	1.454	1.298	1.241	1.403	1.378
F(000)	888	2032	2160	1208	1536
μ (Mo$K\alpha$)/mm^{-1}	0.475	0.384	0.350	0.360	0.296
Measured data	4891	15227	33649	10975	7729
□θ range/°	3.6 – 28.9	3.5 – 29.1	3.3 – 29.0	3.0 – 29.0	3.8 – 28.9
Unique data	2300	10264	12535	6302	4060
Observed data ($I \geq 2.0\sigma(I)$)	1843	6006	8979	4047	2263
No. of parameters	152	663	639	370	244
R, obs. data; all data	0.049; 0.064	0.080; 0.138	0.046; 0.073	0.051; 0.092	0.063; 0.132
a; *b* in weighting scheme	0.065; 1.116	0.120; 0	0.047; 0.005	0.059; 0	0.016; 0
R_w, obs. data; all data	0.127; 0.135	0.194; 0.239	0.092; 0.102	0.112; 0.129	0.070; 0.086
Range of residual electron density peaks/eÅ^{-3}	-0.39 – 0.24	-0.30 – 0.83	-0.20 – 0.28	-0.31 – 0.27	-0.21 – 0.26

[a] The unit cell characteristics do not take into account the unknown solvent within the solvent accessible voids.

Cell culture and *in vitro* cytotoxicity

Ovarian carcinoma A2780 (European Collection of Authenticated Cell Cultures) and colorectal adenocarcinoma HT-29 (American Type Culture Collection) cancer cell lines were cultured as monolayers in Roswell Park Memorial Institute (RPMI) 1640 medium, supplemented with 10% fetal bovine serum, 1% L-glutamine, and 1% Penicillin-Streptomycin (all purchased from Biological Industries), at 37 °C in a 5% CO_2 atmosphere. Cytotoxicity was measured by the previously reported MTT method.[79] In a standard experiment, cells were seeded in 96-well plates at a density of ca. 10000 cells per well and allowed to attach overnight. In the following day, compounds **1**-**6** were dissolved in DMSO (Alfa Aesar) and serially diluted, to create 10 concentrations of each compound, with pure DMSO as the control. The solutions were then diluted further in cell-culture media, to ensure a final concentration of 0.5% DMSO, and added to the cells. The plates were incubated under the previously described conditions for 72 hours, after which MTT (3-(4,5-dimethylthiazol-2-yl)-2,5-diphenyltetrazolium bromide, Sigma Aldrich) was added to the wells (0.1 mg in 20 µL) for an additional 3 hours incubation period. The medium was removed and replaced with 200 µL of isopropanol (Gadot-Group), and upon complete dissolution of the formazan, the absorbance was measured at 550 nm using a Spark 10 M multimode microplate reader spectrophotometer (Tecan Group Ltd., Mannedorf, Switzerland). Each measurement was repeated at least 3 × 3 times: three repeats per plate, all repeated on at least three different days, creating at least nine repetitions for each experiment. The relative IC_{50} values and the standard error of means were determined by a nonlinear regression of a variable slope (four parameters) model using the GraphPad Prism 5.0 software.

Hydrolytic stability

The kinetic hydrolytic stability of **1**-**6** was studied by ^{1}H NMR spectroscopy at 298 K using a Bruker AMX 500 spectrometer, as previously described.[44] For each compound, an initial spectrum was recorded after dissolving the compound and the internal standard, 1,4-dinitrobenzene (Sigma Aldrich), in DMSO-d_6 (Cambridge Isotope Laboratories, Inc.), to produce a ca. 5 mM solution. Afterwards, >1000 equivalents of D_2O (Cambridge Isotope Laboratories, Inc.) were added to create a 9:1 DMSO-d_6/D_2O solution, and a spectrum was recorded immediately. The hydrolytic process was monitored by comparing the integration of a selected ligand peak at a given time point to its original integration upon the addition of D_2O, in relation to the internal standard. Compounds **2**, **3** and **6** were monitored for 24 hours, whereas compounds **1**, **4** and **5** were monitored for 3 hours.

Results and discussion

Synthesis and Characterization

The present investigation includes Schiff base ligands derived from biologically important chiral amino acids for developing potential new titanium(IV)-based anticancer agents. To achieve solubility of the starting materials and *in situ* generated Schiff-base ligands, a benzene/methanol mixture was selected as solvent. Ti(IV) complexes **1**-**6** (Scheme 1) were prepared in one pot reaction by employing the respective chiral amino acid, 2-hydroxybenzaldehyde, and titanium(IV) tetra(isopropoxide) in benzene/methanol. Generally, after 7-8 h {hours are used elsewhere}, the reaction was complete as identified by NMR analysis. The complexes were isolated as orange (**1**-**5**) or red (**6**) crystalline materials and were stable *in vacuo,* but the crystals turned into powder with time. The IR spectra of **1**-**6** show two intense bands in the regions between 1688-1701 and 1393-1402 cm^{-1} corresponding to $\nu(OCO)_{asym}$ and $\nu(OCO)_{sym}$ vibrations, respectively. The observed

differences between the asymmetric and symmetric vibrations were greater than 200 cm^{-1}, indicating a monodentate coordination of the carboxylate ligand;[80] this assumption was subsequently confirmed by the results of single crystal X-ray diffraction studies (*vide infra*). The ^{1}H NMR and $^{13}C\{^{1}H\}$ NMR spectra also supported formation of **1**-**6** (Figures S1-S12).

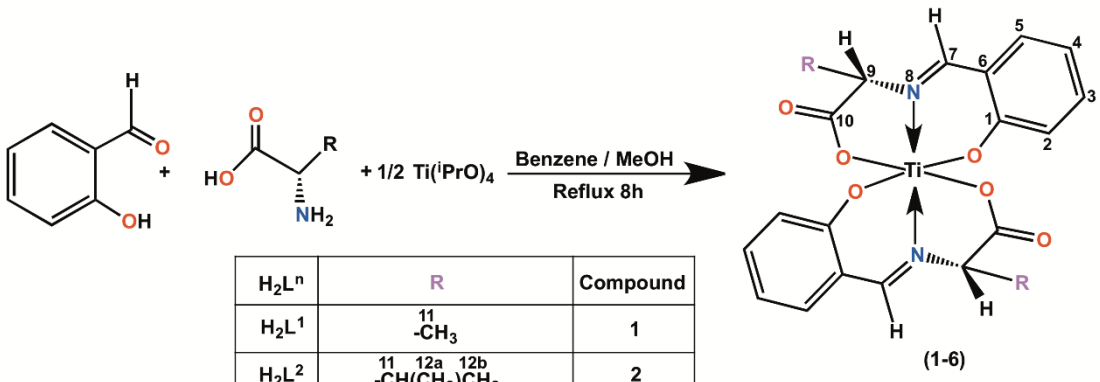

H_2L^n	R	Compound
H_2L^1	^{11}-CH_3	1
H_2L^2	^{11} ^{12a} ^{12b} -$CH(CH_3)CH_3$	2
H_2L^3	^{11} ^{14} ^{12} ^{13} -$CH(CH_3)CH_2CH_3$	3
H_2L^4	^{12} ^{11} ^{13a} ^{13b} -$CH_2CH(CH_3)CH_3$	4
H_2L^5	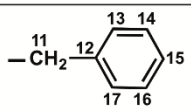	5
H_2L^6	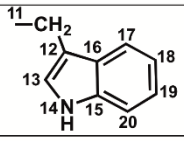	6

Scheme 1. Preparation of titanium(IV) complexes **1**-**6** along with the atom numbering protocol used for NMR signal assignments (see experimental section).

Molecular structures

The molecular structures of **1**-**3**, **5**, and **6** have been established by single crystal X-crystallography and are illustrated in Figure 1, and selected geometric parameters are collated in Table 2. The titanium(IV) center in 1 is located on a crystallographic 2-fold axis of symmetry, indicating that the di-negative anions were strictly equivalent. The tridentate ligand coordinates via carboxylate-O-, imine-N- and phenoxide-O

atoms to establish five- and six-membered chelate rings. The Ti–O1(carboxylate) bond length was significantly longer than the Ti–O3(phenoxide) bond, which correlates with the presence of the electronegative-O2(carbonyl) atom bound to the quaternary-C1 atom. The disparity in the C1–O1, O2 bond lengths, i.e. 1.301(3) and 1.206(3) Å, respectively, clearly indicated a monodentate coordination of the carboxylate ligand. The C4═N1 bond length of 1.281(3) Å was consistent with the presence of an imine bond. The resultant *trans*-N_2O_4 donor set was based on a distorted octahedron with the like atoms being in a *trans* configuration. Both of the *trans* O–Ti–O angles deviated by more than 20° from the ideal 180°. The Ti–O1–C1 [125.50(17)°], Ti–O3–C10 [137.54(15)°], and Ti–N1–C4 [126.76(16)°] angles all exceed 120°, especially the one subtended at the phenoxide-O3 atom. Neither of the five- or six-membered chelate rings was planar. For the former, the r.m.s. deviation of the O1, C1, C2 and N1 atoms was 0.0847 Å. The Ti atom lies 0.150(5) Å out of the plane and may be considered as the flap atom in an envelope conformation. The envelope conformation was more pronounced for the six-membered chelate ring with the r.m.s. deviation for the O3, C10, C5, C4, and N1 atoms being 0.0285 Å and with the Ti atom lying 0.391(3) Å out of the plane. As a first approximation, the tridentate ligand may be considered planar as the dihedral angle formed between the best planes through the chelate rings was 8.50(14)°. Four other structures in the series were obtained. In **2** and **3**, two independent molecules comprise the asymmetric unit, whereas in **6**, the molecule has 2-fold symmetry. Complex **2** has also been characterized previously as a dichloromethane solvate.[81] In this literature structure, designated **2'**, the molecule has 2-fold symmetry.

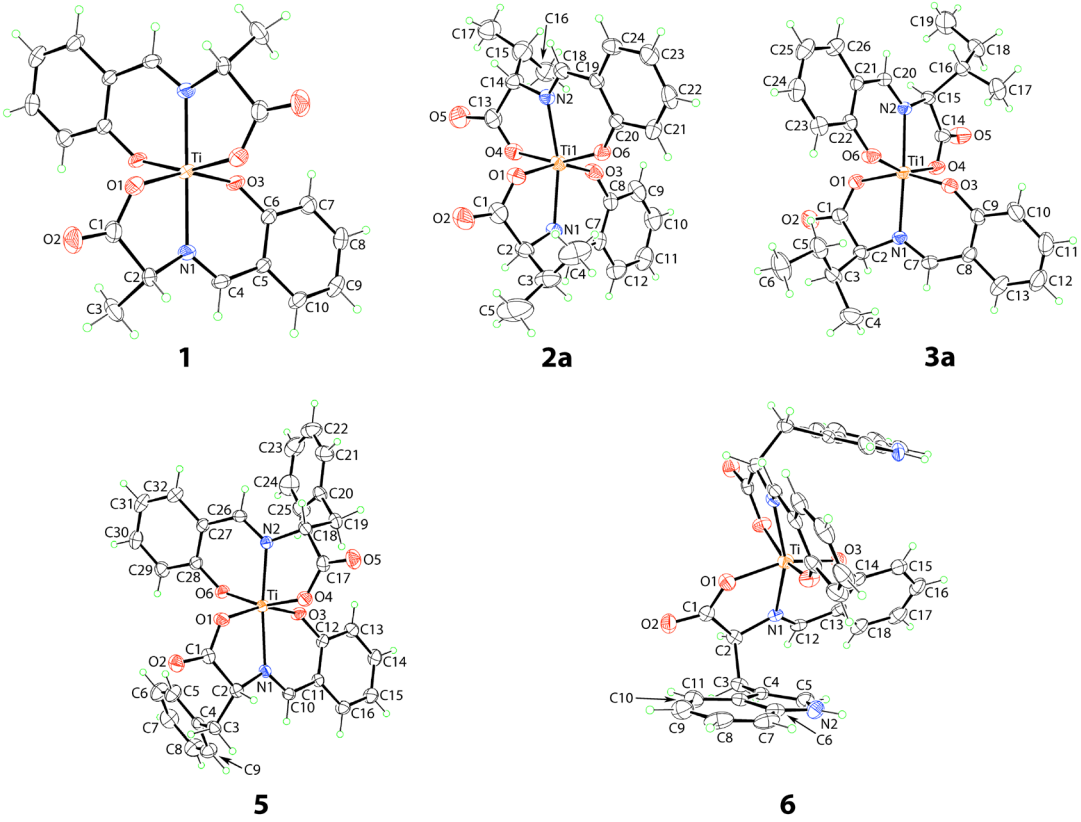

Figure 1. Molecular structures of **1**, **2a** (the imine-C6 atom is obscured), **3a**, **5,** and **6** (benzene molecule omitted) showing atom labeling schemes and anisotropic displacement parameters at the 25% probability level (refer to Figure S13 for **2b** and **3b**). The titanium atom in each of **1** and **6** lies on a crystallographic 2-fold axis of symmetry. Unlabeled atoms are related by the symmetry operation 1-x, y, 1½-z (**1**) and 1-y, 1-x, ½-z (**6**).

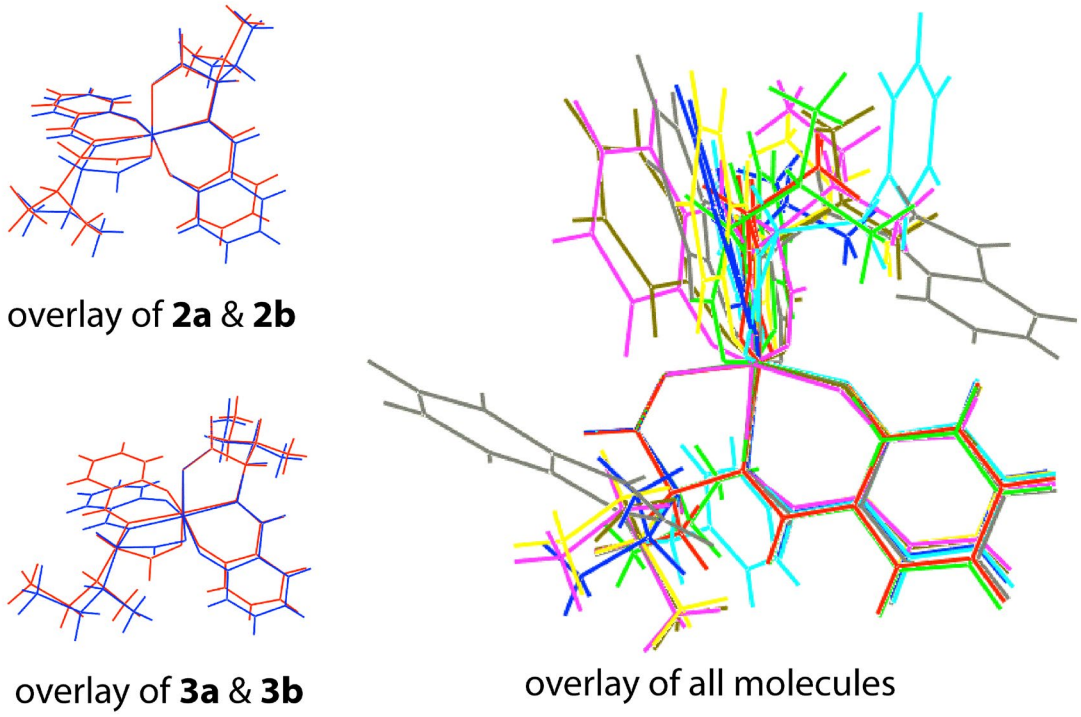

Figure 2. Overlay diagrams showing molecules of **2a** (red image) and **2b** (inverted, blue), molecules of **3a** (red image) and **3b** (blue), and of all molecules: **1** (red image), **2a** (blue), **2b** (inverted; green), **3a** (pink), **3b** (yellow), **5** (aqua), **6** (grey) and **2'** (Hu 2001,[73] olive green); molecules have been overlapped so that one of the carboxylate residues in each molecule is coincident.

Table 2. Selected geometric parameters (Å, °) for complexes **1**-**3**, **5**, and **6**.

Complex Parameter	**1**[a]	**2a**	**2b**[b]	**3a**	**3b**[b]	**5**	**6**[a]
Ti–O1	1.946(2)	1.934(5)	1.931(6)	1.953(2)	1.940(2)	1.9199(17)	1.946(3)
Ti–O3	1.850(2)	1.847(5)	1.838(6)	1.857(2)	1.842(2)	1.8345(16)	1.840(3)
Ti–N1	2.140(2)	2.159(6)	2.155(7)	2.143(3)	2.141(3)	2.1573(18)	2.140(3)
Ti–O4	1.946(2)	1.922(6)	1.936(6)	1.939(2)	1.951(2)	1.9382(17)	1.946(3)
Ti–O6	1.850(2)	1.853(5)	1.849(7)	1.846(2)	1.840(2)	1.8455(16)	1.840(3)
Ti–N2	2.140(2)	2.147(6)	2.147(7)	2.154(3)	2.146(3)	2.1145(18)	2.140(3)
O1–Ti–O3	159.13(7)	158.3(3)	157.8(3)	158.1(1)	159.1(1)	158.51(7)	158.9(1)
O1–Ti–O3	89.6(1)	88.1(2)	90.6(3)	90.8(1)	88.2(1)	91.28(8)	91.0(2)
O1–Ti–N1	75.72(7)	76.2(2)	75.6(3)	75.2(1)	75.8(1)	75.92(7)	75.7(1)
O3–Ti–N1	83.52(7)	82.2(2)	82.6(3)	82.9(1)	83.3(1)	82.94(7)	83.4(1)
O4–Ti–O6	159.13(7)	158.3(3)	157.8(3)	158.2(1)	158.6(1)	157.56(7)	158.9(1)
O4–Ti–N2	75.72(7)	76.1(2)	75.7(3)	75.8(1)	75.9(1)	75.62(7)	75.7(1)
O6–Ti–N2	83.52(7)	82.3(2)	82.1(3)	82.5(1)	82.7(1)	82.22(7)	83.4(1)
N1–Ti–N2	169.63(1)	165.4(2)	164.0(2)	164.4(1)	165.5(1)	167.52(7)	159.8(2)

[a] The molecule in each of **1** and **6** has crystallographic 2-fold symmetry so both ligands have identical parameters. [b] For **2b** and for **3b**, add “6” to the atom labels for the oxygen atoms and “2” for nitrogen atoms.

The independent molecules in **2**, i.e. **2a** and **2b**, differed non-trivially, exhibiting differences in the relative orientations of the peripheral groups as may be seen from the overlay diagram in Figure 2; the same comments pertain to the two molecules in **3**. Despite these differences, no systematic trends between **2a** and **2b** nor between **3a** and **3b** were evident in terms of the derived interatomic parameters, Table 2 and ESI Table S1. Across the series, the most planar five-membered chelate ring was found for the O1-ring in **2b** while the most distorted was found in **1** (both rings). For the six-membered chelate rings, the most planar was found in **2a** (O3-ring) and the most distorted in **5** (O4-ring, second molecule). In terms of deviations of the titanium atom from the planes of the other atoms comprising the five-membered rings, the metal was close to co-planar with the four atoms in **6** (O3-ring) and exhibited the greatest deviation in **5** (O4-ring, second molecule), see ESI Table S1. The minimum and maximum deviations of the titanium atom from the five other atoms of the six-membered chelate rings was found in **2a** (O3-ring) and **5** (O3-ring), respectively. No systematic variations in the geometric parameters were evident across the series of molecules. In terms of the dihedral angles between the chelate rings, the greatest dihedral angle of 17.51(10)° was found for one of the ligands in **5** and the smallest, i.e. 2.64(8)°, was also found in **5**. The conformational flexibility in this series of structures is highlighted in the overlay diagrams of Figure 2.

An important aspect of the crystallographic analysis worth commenting upon is the apparent racemization that has occurred during crystallization. The syntheses were conducted on authenticated chiral Schiff bases derived from various amino acids. Crystals of **1** and **5** were found to adopt centrosymmetric space groups, whereas those of **2**, **3**, and **6** were found in chiral space groups. Similar behavior was noted in the crystal chemistry of several diorganotin(IV) Schiff base derivatives derived from L-tyrosine.[82]

One other crystalline sample was obtained, namely of compound **4**, but unresolvable issues in the refinement precluded detailed reporting of the structure.[83] The

preliminary structural study of **4**, derived from L-leucine, suggested that five independent molecules comprised the asymmetric unit, and each of these also adopted the isomeric form akin to **2a**. Also noteworthy is that **4** crystallized in the non-centrosymmetric space group $P2_12_12_1$.

Molecular packing

In the absence of conventional hydrogen bonding interactions, molecules in the crystals of **1**-**3** and **5** were connected by various non-covalent interactions, whereas conventional N–H···O hydrogen bonding was noted in the crystal of **6**. The geometric parameters characterizing the specified intermolecular interactions in the following discussion are collated in the respective figure captions (ESI Figures S14-S18).

In the molecular packing of **1**, molecules were connected into supramolecular layers in the bc-plane by π-stacking between phenyl rings as well as methine-C–H···π(phenyl) interactions. The carbonyl-O2 atoms protruded to either side of the layer (ESI Figure S14a), and these were pivotal in linking layers along the a-axis via methyl- and phenyl-C–H···O(carbonyl) interactions (see ESI Figure S14b for the unit cell contents of **1**). In the crystal of **2**, similar interactions were evident between the independent molecules: π-stacking between the phenyl rings, combined with phenyl-C–H···π(phenyl) and imine-C–H···O(carbonyl) interactions, which lead to the formation of supramolecular chains along the c-axis (ESI Figure S15a). The chains were linked into a three dimensional architecture by phenyl-C–H···O(carbonyl) contacts (see ESI Figure S15b for the unit cell contents of **2**). Similar types of contacts pertained in the crystal of **3**, which accommodated an undetermined solvent in the voids defined by the complex molecules. Contacts of the type imine-, methyl-, and phenyl-C–H···O(carbonyl), π(phenyl)···π(phenyl), and phenyl-C–H···π(phenyl), linked the molecules into a three dimensional architecture (ESI Figure S16).

Supramolecular layers parallel to (-1 0 1) were evident in the molecular packing of **5** (ESI Figure S17a). The connections between the molecules were of the type imine-,

phenyl-, and methylene-C–H···O(carbonyl), methane-C–H···π(phenyl), and carbonyl-C=O···π(phenyl). While not common, carbonyl-C=O···π(phenyl) and related O(lone-pair)···π(arene) interactions are known to be important in assembling molecules in crystals.[84-86] In the present case and as illustrated in Figure 3, centrosymmetric, supramolecular dimers formed, which is the commonly adopted motif stabilized by such interactions. In the crystal of **5**, layers stacked without directional interactions between them (see ESI Figure S17b for the unit cell contents of **5**). In the crystal of **6**, both complex and solvent (benzene) molecules were present, in a 1:1 ratio, and a 1H-indolyl residue presented the opportunity for conventional hydrogen bonding. Indeed, weak indolyl-N–H···O(carboxylate) hydrogen bonding was observed and as, from symmetry, each complex molecule formed two donor and two acceptor interactions, the hydrogen bonding served to stabilize the three dimensional architecture. Supporting phenyl-C–H···O(carbonyl) and phenyl-C–H···π(phenyl) interactions contributed to the stability of the molecular packing. The solvent benzene molecules resided in channels along the a-axis direction with no directional interactions between the complex and solvent molecules (see ESI Figure S18 for the unit cell contents of **6**).

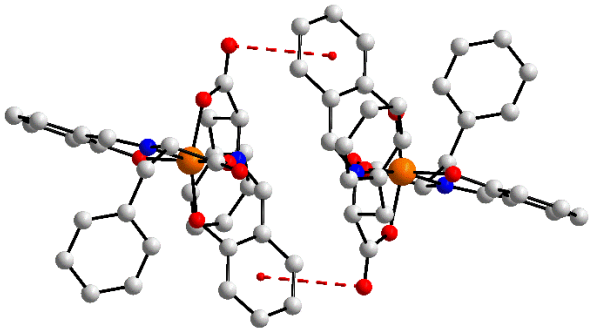

Figure 3. Supramolecular aggregate in the crystal of **5** stabilized by carbonyl-C=O···π(phenyl) interactions, shown as red dashed lines. For reasons of clarity, non-participating hydrogen atoms are removed.

Photophysical properties

The photophysical properties and the fluorescent processes have been reviewed recently which are largely concentrated on the complexes of mid to late transition metals.[87] With the well-characterized series of octahedral titanium(IV) complexes (**1**-**6**) in hand, their photophysical properties were of interest. Representative spectral profile of **1**-**6** in solution and in the solid state is depicted in Figure 4. The absorption spectra of the compounds in acetonitrile and DMSO solutions show two peaks centered at ~300 and ~360 nm. The absorption spectral profile was particularly insensitive to the nature of substitution of the ligand (Figure 4(a)). Excitation at 300 nm produced a broad and unstructured emission at 390 nm for most of the complexes in acetonitrile, with exception of **1** and **3**, in which the fluorescence peak appeared at 440 nm (Figure 4(b)). However, excitation at the lower energy absorption band (360 nm) produced a very broad emission band within the 390–540 nm range, with a peak position at 440 nm (Figure 4(d)). The spectral peak positions for **1**-**6** along with the calculated fluorescence yields (ϕ_f) in acetonitrile are given in Table 3. Fluorescence relaxation dynamics in a nanosecond time domain was also measured in acetonitrile exciting by 295 and 365 nano-LED and monitoring the emission at the respective fluorescence maximum (Figures 4(e) and 4(f)). The fluorescence decays were mostly non exponential in both cases. Individual contribution of different decay components in each case is also incorporated in Table 3. At 295 nm excitation, the fastest decay component (τ1 = 0.5-1.5 ns) contributed the most (50-90%), while the long decay component (τ3 > 5.0 ns) showed an insignificant contribution (only 5-10%). Overall, the average fluorescence decay time (τ_{avg}) for the complexes was within 3.2-4.6 ns for the 340 nm emission (λ_{ex} = 295 nm), whereas the corresponding decay time of 0.5-1.2 ns was observed for the 440 nm emission (λ_{ex} = 365 nm). Interestingly, the photoluminescence behavior is strikingly different for the complexes when measured in DMSO solution. The principle

fluorescence peaks for the complexes appeared at 440 nm when excited at 300 and 360 nm (Figure 4(c)). The 340 nm emission appeared as a mere hump when the fluorescence emission was collected by excitation at 300 nm. The spectral behavior along with the details of time resolved measurements for **1**-**6** in DMSO are provided in ESI Figure S19 and ESI Table S2. Notably, the average fluorescence lifetime of 440 nm emission increased significantly (τ_{avg} = 2.7-4.8 ns) in the DMSO solution. The solid-state photoluminescence spectra of **1**-**6** displayed a broad band in the ~550-570 nm region (Figure 4(g)). The bi-exponential fluorescence decay kinetics (Figure 4(h)) comprised a major component with a very fast time constant of 600-700 ps, and a very small contribution (<1%) with a lifetime of 7-9 ns (Table 3). The average fluorescence decay time in the solid state (0.6-1.0 ns) was much faster than in solution, which signifies appreciable stabilization of the excited state in the latter case.

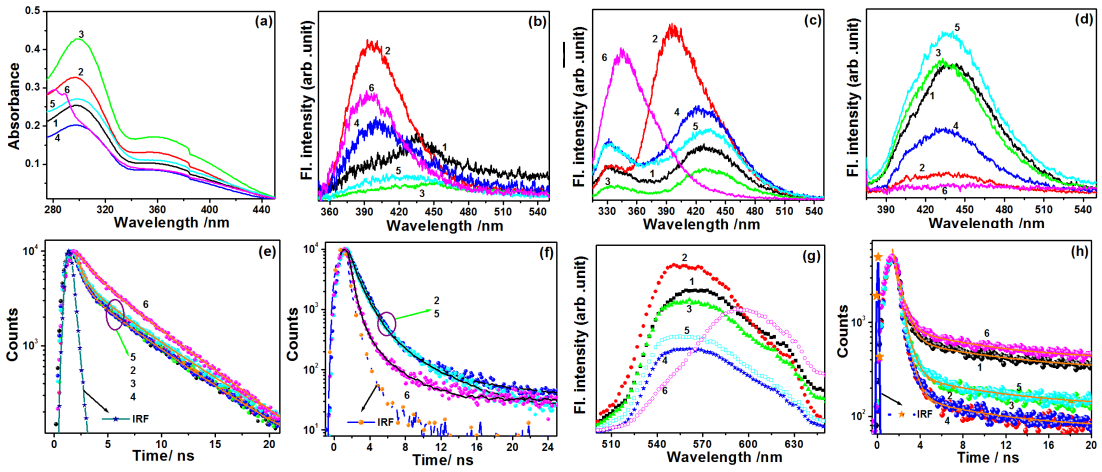

Figure 4. Photophysical properties of **1**-**6** at various experimental conditions. Absorption spectra (a). Emission spectra; λ_{ex} = 295 nm in acetonitrile (b) λ_{ex} = 295 nm in DMSO (c) and λ_{ex}= 365 nm in acetonitrile (d). Fluorescence decay traces in acetonitrile excited at 295 nm (e) and 365 nm (f). Fluorescence emission (g) and time-resolved fluorescence decay (h) of **1**-**6** in the solid state.

Table 3. Photophysical parameters for **1-6** in acetonitrile solution and in solid state.

Steady state				
Complex	**In acetonitrile**			**In solid-state**
	$^{max}\lambda_{abs}$ /nm	**$^{max}\lambda_{em}$ /nm**	**ϕ_f**	**$^{max}\lambda_{em}$ /nm**
1	297, 363	440	0.011	566
2	297, 369	434	0.002	558
3	300, 366	433	0.008	561
4	297, 365	434	0.007	559
5	297, 364	437	0.014	557
6	297 ,360	434	0.002	595

Time resolved fluorescence decay in acetonitrile												
	λ_{ex}: 295 nm; λ_{mon}: 340 nm							**λ_{ex}: 365 nm; λ_{mon}: 435 nm**				
	α_1 (%)	**τ_1 /ns**	**α_2 (%)**	**τ_2 /ns**	**α_3 (%)**	**τ_3 /ns**	**τ_{av} ns**	**α_1 (%)**	**τ_1 /ns**	**α_2 (%)**	**τ_2 /ns**	**τ_{av} /ns**
1	75.45	0.56	14.77	3.76	9.82	6.84	4.20	88.47	1.38	11.53	4.28	2.21
2	87.11	0.86	12.89	5.70			3.25	85.02	0.98	14.98	2.10	1.29
3	79.53	0.71	20.47	5.66			4.03	93.85	1.01	6.15	4.41	1.77
4	76.78	0.57	18.28	4.47	4.95	8.13	4.34	76.93	0.15	23.04	1.57	1.22
5	72.79	0.55	15.99	3.92	11.22	7.11	4.57	79.53	0.28	20.47	1.82	1.24
6	48.28	1.47	51.72	5.21			4.43	99.31	0.21	0.69	2.75	0.42

Time resolved fluorescence decay in the solid state; λ_{ex}: 365 nm; λ_{mon}: 560-590 nm					
	α_1 (%)	**τ_1 /ns**	**α_2 (%)**	**τ_2 /ns**	**τ_{av} /ns**
1	99.74	0.69	0.13	9.46	0.84
2	99.87	0.60	0.13	9.20	0.77
3	99.75	0.64	0.25	10.06	1.00
4	99.86	0.60	0.14	7.47	0.72
5	99.74	0.63	0.26	8.52	0.90
6	99.97	0.69	0.26	10.04	1.03

Cytotoxicity and hydrolytic stability

The cytotoxicity of **1**-**6** toward two human cancer cell lines, the ovarian carcinoma A2780 and the colorectal adenocarcinoma HT-29, was assessed by the previously reported MTT (3-(4,5-dimethylthiazol-2-yl)-2,5-diphenyltetrazolium bromide) assay.[79] The dose response curves are depicted in Figure 5, and the relative IC_{50} values are summarized in Table 4.

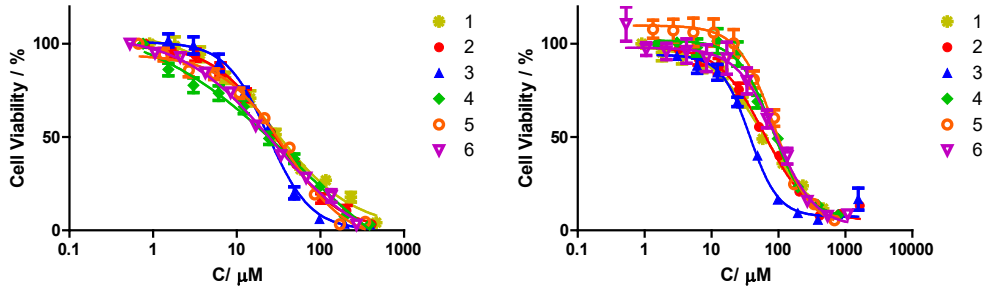

Figure 5. Dependence of A2780 (left) and HT-29 (right) cell viability on the administered concentration of **1**-**6**, as measured by the MTT assay following a three day incubation period.

Table 4. IC_{50} values toward the human A2780 and HT-29 cancer cell lines, and $t_{1/2}$ for hydrolysis values of **1**-**6**.

Complex	**IC_{50} (µM)**		**$t_{1/2}$ for hydrolysis (hours)**
	A2780	**HT-29**	
1	30 ± 8	60 ± 10	0.7 ± 0.1
2	28 ± 2	60 ± 3	9.5 ± 0.4
3	23 ± 2	36.2 ± 0.4	15 ± 2
4	48 ± 3	81 ± 4	1.18 ± 0.05
5	37 ± 7	89 ± 9	1.67 ± 0.07
6	29 ± 3	103 ± 9	5.7 ± 0.1

All tested compounds were cytotoxic, with similar reactivity toward both lines. As expected, the ovarian line was more sensitive than the colorectal line for all

compounds tested.[31,48] The IC_{50} values were mostly in the same order of magnitude as those obtained for cisplatin,[88] or one order higher, with **3** as the most potent compound toward both cell lines.

The comparative hydrolytic stability of **1**-**6** was assessed by ^1H NMR, with 1,4-dinitrobenzene as an internal standard, as previously described.[44] The half-life values toward hydrolysis upon the addition of 10% D_2O are summarized in Table 4 (See ESI Figures S20 and S21). Whereas **1**, **4**, and **5** exhibited relatively low stabilities, with $t_{1/2}$ values of around 1 h, compounds **2**, **3**, and **6** were stable for longer periods, up to $t_{1/2}$ of 15 h for the most stable compound, **3**. These stabilities are lower than those previously obtained for related systems that are based on phenolato/alkoxo ligands.[29,34,44,49,51,54] This may be attributed to weaker binding of the carboxylate ligand, as observed previously.[89]

Inspecting the overall data, **3** is identified as both the most active and the most stable of the six compounds. The high stability may be attributed to the larger steric bulk, inhibiting interactions with water molecules.[39,44,47] This hypothesis is further supported when inspecting other complexes, whereby larger steric bulk near the metal center translates to higher stability, with lowest stability for the smallest methylated compound **1**. Nevertheless, no clear correlation between activity and stability is detected for the rest of the complexes, and especially as some highly unstable complexes are still cytotoxic, it is reasonable that hydrolysis products may serve as active species in the cell, as reported previously.[34,35,39,42,90] It is possible that the least stable **1**, featuring smallest steric bulk, may yield small enough hydrolysis products that can penetrate through the cell membrane and demonstrate activity. Interestingly, **2**, **3**, and **6** were more soluble in DMSO than **1**, **4**, and **5**, which correlates with their higher stability, but not necessarily higher cytotoxicity.

Conclusions

Six titanium(IV) complexes based on tridentate *ONO*-type Schiff base ligands derived from chiral amino acids were synthesized and fully characterized. X-ray crystallography established a *trans*-N_2O_4 donor set defined by carboxylate-O-, imine-N- and phenoxide-O atoms of two di-anionic, tridentate ligands. Photoluminescence behavior of the complexes was significantly different in DMSO and in acetonitrile. Further, excited state relaxation was much faster in the solid state than in solution. These complexes represent a new family of anticancer Ti(IV) compounds, with marked activity toward colon and ovarian human cancer cell lines.[48] Similar ligands to those used herein were previously employed on metals such as Sn(IV), resulting in highly antineoplastic compounds.[70-71] The mediocre hydrolytic stability recorded for the complexes implies that some hydrolysis takes place in the cellular environment, and additional studies are required to fully elucidate the nature of the active species.

Acknowledgments

Funding was received from the European Research Council (ERC) under the European Union's Horizon 2020 research and innovation programme (grant agreement 681243). Additionally, financial support from the University Grants Commission, India (Grant No. 42-396/2013 (SR), 2013, TSBB) and the University Grants Commission, India through SAP-CAS, Phase-I (Grant No. F 540/21/CAS/2013 (SAP-I) are gratefully acknowledged. TSBB and RM acknowledge DST-PURSE for the diffractometer facility.

References

[1] K. D. Mjos, C. Orvig, *Chem. Rev.* **2014**, *114*, 4540–4563.

[2] D. Wang, S. J. Lippard, *Nat. Rev. Drug Discov.* **2005**, *4*, 307–320.

[3] S. Dilruba, G. V. Kalayda, *Cancer Chemother. Pharmacol.* **2016**, *77*, 1103–1124.

[4] P. Köpf-Maier, H. Köpf, *Chem. Rev.* **1987**, *87*, 1137–1152.

[5] E. Meléndez, *Crit. Rev. Oncol. Hematol.* **2002**, *42*, 309–315.

[6] P. M. Abeysinghe, M. M. Harding, *Dalton Trans.* **2007**, 3474–3482.

[7] I. Ott, R. Gust, *Arch. Pharm.* **2007**, *340*, 117–126.

[8] K. Strohfeldt, M. Tacke, *Chem. Soc. Rev.* **2008**, *37*, 1174–1187.

[9] E. Y. Tshuva, D. Peri, *Coord. Chem. Rev.* **2009**, *253*, 2098–2115.

[10] I. Kostova, *Anticancer. Agents Med. Chem.* **2009**, *9*, 827–842.

[11] E. Y. Tshuva, J. A. Ashenhurst, *Eur. J. Inorg. Chem.* **2009**, 2203–2218.

[12] K. M. Buettner, A. M. Valentine, *Chem. Rev.* **2012**, *112*, 1863–1881.

[13] Y. Ellahioui, S. Prashar, S. Gómez-Ruiz, *Inorganics* **2017**, *5*, 4–27.

[14] S. A. Loza-Rosas, M. Saxena, Y. Delgado, K. Gaur, M. Pandrala, A. D. Tinoco, *Metallomics* **2017**, *9*, 346–356.

[15] M. E. Heim, H. Flechtner, B. K. Keppler, in *Ruthenium and Other Non-Platinum Metal Complexes in Cancer Chemotherapy*. *Progress in Clinical Biochemistry and Medicine*, Vol. 10 (Eds.: E. Baulieu, D. T. Forman, M. Ingelman-Sundberg, L. Jaenicke, J. A. Kellen, Y. Nagai, L. Träger, L. Will-Shahab, J. L. Wittliff), Springer, Berlin, Heidelberg, **1989**, pp. 217–223.

[16] M. Cini, T. D. Bradshaw, S. Woodward, *Chem. Soc. Rev.* **2017**, *46*, 1040–1051.

[17] E. Y. Tshuva, M. Miller, in *Metallo-Drugs: Development and Action of Anticancer Agents*. *Metal Ions in Life Sciences*, Vol. 18 (Eds.: A. Sigel, H. Sigel, E. Freisinger, R.K.O. Sigel), De Gruyter, Berlin, **2018**, pp. 219–249.

[18] B. K. Keppler, C. Friesen, H. G. Moritz, H. Vongerichten, E. Vogel, in *Bioinorganic Chemistry. Structure and Bonding*, Vol. 78, Springer, Berlin,

Heidelberg, **1991**, pp. 97-127.

[19] T. Schilling, K. B. Keppler, M. E. Heim, G. Niebch, H. Dietzfelbinger, J. Rastetter, A. R. Hanauske, *Investig. New Drugs* **1996**, *13*, 327–332.

[20] C. Christodoulou, A. Eliopoulos, L. Young, L. Hodgkins, D. Ferry, D. Kerr, *Br. J. Cancer* **1998**, *77*, 2088–2097.

[21] A. Korfel, M. E. Scheulen, H. J. Schmoll, O. Gründel, A. Harstrick, M. Knoche, L. M. Fels, M. Skorzec, F. Bach, J. Baumgart, G. Sass, S. Seeber, E. Thiel, W. E. Berdel, *Clin. Cancer Res.* **1998**, *4*, 2701–2708.

[22] G. Lümmen, H. Sperling, H. Luboldt, T. Otto, H. Rübben, *Cancer Chemother. Pharmacol.* **1998**, *42*, 415–417.

[23] N. Kröger, U. R. Kleeberg, K. Mross, L. Edler, D. K. Hossfeld, *Oncol. Res. Treat.* **2000**, *23*, 60–62.

[24] F. Caruso, M. Rossi, C. Pettinari, *Expert Opin. Ther. Pat.* **2001**, *11*, 969–979.

[25] K. Mross, P. Robben-Bathe, L. Edler, J. Baumgart, W. E. Berdel, H. Fiebig, C. Unger, *Onkologie* **2000**, *23*, 576-579.

[26] J. H. Toney, T. J. Marks, *J. Am. Chem. Soc.* **1985**, *107*, 947–953.

[27] F. Caruso, L. Massa, A. Gindulyte, C. Pettinari, F. Marchetti, R. Pettinari, M. Ricciutelli, J. Costamagna, J. C. Canales, J. Tanski, M. Rossi, *Eur. J. Inorg. Chem.* **2003**, *2003*, 3221–3232.

[28] M. Shavit, D. Peri, C. M. Manna, J. S. Alexander, E. Y. Tshuva, *J. Am. Chem. Soc.* **2007**, *129*, 12098–12099.

[29] D. Peri, S. Meker, C. M. Manna, E. Y. Tshuva, *Inorg. Chem.* **2011**, *50*, 1030–1038.

[30] T. A. Immel, M. Debiak, U. Groth, A. Bürkle, T. Huhn, *ChemMedChem* **2009**, *4*, 738–741.

[31] M. Miller, O. Braitbard, J. Hochman, E. Y. Tshuva, *J. Inorg. Biochem.* **2016**, *163*, 250–257.

[32] A. Tzubery, E. Y. Tshuva, *Eur. J. Inorg. Chem.* **2017**, *2017*, 1695–1705.

[33] M. Miller, E. Y. Tshuva, *Eur. J. Inorg. Chem.* **2014**, *2014*, 1485–1491.

[34] M. Miller, E. Y. Tshuva, *Sci. Rep.* **2018**, *8*, 9705.

[35] C. M. Manna, G. Armony, E. Y. Tshuva, *Chem. - A Eur. J.* **2011**, *17*, 14094–14103.

[36] C. M. Manna, E. Y. Tshuva, *Dalton Trans.* **2010**, *39*, 1182–1184.

[37] H. Glasner, E. Y. Tshuva, *J. Am. Chem. Soc.* **2011**, *133*, 16812–16814.

[38] H. Glasner, E. Y. Tshuva, *Inorg. Chem.* **2014**, *53*, 3170–3176.

[39] S. Meker, C. M. Manna, D. Peri, E. Y. Tshuva, *Dalton Trans.* **2011**, *40*, 9802-9809.

[40] D. Peri, C. M. Manna, M. Shavit, E. Y. Tshuva, *Eur. J. Inorg. Chem.* **2011**, *2011*, 4896–4900.

[41] A. Tzubery, E. Y. Tshuva, *Inorg. Chem.* **2011**, *50*, 7946–7948.

[42] A. Tzubery, E. Y. Tshuva, *Inorg. Chem.* **2012**, *51*, 1796–1804.

[43] S. Barroso, A. M. Coelho, S. Gómez-Ruiz, M. J. Calhorda, Ž. Žižak, G. N. Kaluđerović, A. M. Martins, *Dalton Trans.* **2014**, *43*, 17422–17433.

[44] D. Peri, S. Meker, M. Shavit, E. Y. Tshuva, *Chem. - A Eur. J.* **2009**, *15*, 2403–2415.

[45] C. M. Manna, O. Braitbard, E. Weiss, J. Hochman, E. Y. Tshuva, *ChemMedChem* **2012**, *7*, 703–708.

[46] T. A. Immel, U. Groth, T. Huhn, P. Öhlschläger, *PLoS One* **2011**, *6*, 1–7.

[47] T. A. Immel, U. Groth, T. Huhn, *Chem. - A Eur. J.* **2010**, *16*, 2775–2789.

[48] S. Meker, O. Braitbard, M. D. Hall, J. Hochman and E. Y. Tshuva, *Chem. - A Eur. J.*, 2016, **22**, 9986–9995.

[49] S. Meker, K. Margulis-Goshen, E. Weiss, S. Magdassi, E. Y. Tshuva, *Angew. Chem. Int. Ed.* **2012**, *51*, 10515–10517.

[50] S. Meker, K. Margulis-Goshen, E. Weiss, O. Braitbard, J. Hochman, S. Magdassi, E. Y. Tshuva, *ChemMedChem* **2014**, *9*, 1294–1298.

[51] S. Meker, O. Braitbard, K. Margulis-Goshen, S. Magdassi, J. Hochman, E.

Tshuva, *Molecules* **2015**, *20*, 18526–18538.

[52] N. Ganot, O. Briaitbard, A. Gammal, J. Tam, J. Hochman, E. Y. Tshuva, *ChemMedChem* **2018**, *13*, 2290–2296.

[53] M. Grützke, T. Zhao, T. A. Immel, T. Huhn, *Inorg. Chem.* **2015**, *54*, 6697–6706.

[54] T. A. Immel, M. Grützke, A.-K. Späte, U. Groth, P. Öhlschläger, T. Huhn, *Chem. Commun.* **2012**, *48*, 5790–5792.

[55] A. D. Tinoco, H. R. Thomas, C. D. Incarvito, A. Saghatelian, A. M. Valentine, *Proc. Natl. Acad. Sci. U. S. A.* **2012**, *109*, 5016–5021.

[56] R. Manne, M. Miller, A. Duthie, M. F. C. Guedes da Silva, E. Y. Tshuva, T. S. Basu Baul, *Dalton Trans.* **2019**, *48*, 304–314.

[57] K. Severin, R. Bergs, W. Beck, *Angew. Chem. Int. Ed. Engl.* **1998**, *37*, 1634–1654.

[58] D. R. Williams, *Inorganica Chim. Acta Rev.* **1972**, *6*, 123–133.

[59] Y. Tsukada, Y. Nagata, T. Matsutani, T. Matsutani, *J. Neurochem.* **1963**, *10*, 241–256.

[60] Y. Ohsumi, Y. Anraku, *J. Biol. Chem.* **1981**, *256*, 2079–2082.

[61] G. A. Rosenthal, *Life Sci.* **1997**, *60*, 1635–1641.

[62] M. H. Richmond, *Bacteriol. Rev.* **1962**, *26*, 398–420.

[63] G. S. Ahluwalia, J. L. Grem, Z. Hao, D. A. Cooney, *Pharmacol. Ther.* **1990**, *46*, 243–271.

[64] P. Köpf-Maier, I. C. Tornieporth-Oetting, *BioMetals* **1996**, *9*, 267–271.

[65] H. L. Singh, J. Singh, *Int. J. Inorg. Chem.* **2013**, DOI: 10.1155/2013/847071.

[66] K. H. Puthraya, T. S. Srivastava, A. J. Amonkar, M. K. Adwankar, M. P. Chitnis, *J. Inorg. Biochem.* **1985**, *25*, 207–215.

[67] Y. K. Yan, M. Melchart, A. Habtemariam, P. J. Sadler, *Chem. Commun.* **2005**, 4764–4776.

[68] D. Dakternieks, T. S. Basu Baul, S. Dutta, E. R. T. Tiekink, *Organometallics*

1998, *17*, 3058–3062.

[69] T. S. Basu Baul, C. Masharing, G. Ruisi, R. Jirásko, M. Holčapek, D. de Vos, D. Wolstenholme, A. Linden, *J. Organomet. Chem.* **2007**, *692*, 4849–4862.

[70] T. S. Basu Baul, S. Basu, D. De Vos, A. Linden, *Invest. New Drugs* **2009**, *27*, 419–431.

[71] T. S. Basu Baul, P. Kehie, A. Duthie, N. Guchhait, N. Raviprakash, R. B. Mokhamatam, S. K. Manna, N. Armata, M. Scopelliti, R. Wang, U. Englert, *J. Inorg. Biochem.* **2017**, *168*, 76–89.

[72] Agilent Technologies, CrysAlisPro, Santa Clara, CA (USA), **2013**.

[73] G. M. Sheldrick, *Acta Crystallogr. Sect. A: Found. Adv.* **2008**, *64*, 112–122.

[74] G. M. Sheldrick, *Acta Crystallogr. Sect. C: Struct. Chem.* **2015**, *71*, 3–8.

[75] O. V. Dolomanov, L. J. Bourhis, R. J. Gildea, J. A. K. Howard, H. Puschmann, *J. Appl. Crystallogr.* **2009**, *42*, 339–341.

[76] L. J. Farrugia, *J. Appl. Crystallogr.* **2012**, *45*, 849–854.

[77] DIAMOND, Visual Crystal Structure Information System, Version 3.1, CRYSTAL IMPACT, Postfach 1251, D-53002, Bonn (Germany), **2006**.

[78] A. L. Spek, *Acta Crystallogr. Sect. D Biol. Crystallogr.* **2009**, *65*, 148–155.

[79] N. Ganot, S. Meker, L. Reytman, A. Tzubery, E. Y. Tshuva, *J. Vis. Exp.* **2013**, e50767.

[80] G. B. Deacon, R. J. Phillips, *Coord. Chem. Rev.* **1980**, *33*, 227–250.

[81] C. Hu, W. Zhang, Y. Xu, H. Zhu, X. Ren, C. Lu, Q. Meng, H. Wang, *Transit. Met. Chem.* **2001**, *26*, 700–703.

[82] T. S. Basu Baul, P. Kehie, A. Duthie, R. Wang, U. Englert, H. Höpfl, *J. Organomet. Chem.* **2017**, *828*, 96–105.

[83] Crystal data for 4: $C_{26}H_{30}N_2O_6Ti$, orthorhombic, space group P212121, a = 12.7269(9), b = 17.0641(9), c = 63.245(6) Å, V = 13735.2(17), Z = 20.

[84] E. R. T. Tiekink, *Coord. Chem. Rev.* **2017**, *345*, 209–228.

[85] J. Zukerman-Schpector, I. Haiduc, E. R. T. Tiekink, *Chem. Commun.* **2011**,

47, 12682-12684.

[86] J. Zukerman-Schpector, E. R. T. Tiekink, *CrystEngComm* **2014**, *16*, 6398–6407.

[87] Y. Y. Chia, M. G. Tay, *Dalton Trans.* **2014**, *43*, 13159 –13168.

[88] L. Reytman, O. Braitbard, J. Hochman, E. Y. Tshuva, *Inorg. Chem.* **2016**, *55*, 610–618.

[89] M. Shavit, E. Y. Tshuva, *Eur. J. Inorg. Chem.* **2008**, *2008*, 1467–1474.

[90] C. M. Manna, G. Armony, E. Y. Tshuva, *Inorg. Chem.* **2011**, *50*, 10284–10291.

TOC:

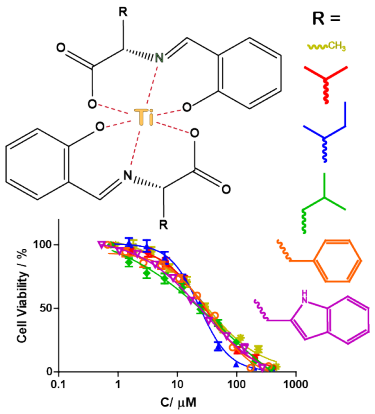

Six homoleptic Ti(IV) complexes containing amino-acid tethered phenolato ligands were synthesized and characterized spectroscopically and crystallographically. The complexes displayed marked cytotoxicity toward human ovarian and colon cancer cells, with mediocre stability in 10% D_2O solutions, overall pointing to steric bulk as a contributor to stability and solubility.